

Marek St. Węglowski, Carter Hamilton

## Investigation into friction stir processing (FSP) of surface layers

### Introduction

Increasing demands for operating properties of fabricated elements on one hand, and a necessity of reducing mass of a structure on the other, triggers materials engineering research into producing surface layers representing required functional properties. Methods commonly used in the production of surface layers, such as surfacing, spraying or re-melting with a laser beam have been known for years. A new method, so far little known in Poland, is the friction stir processing (FSP) of surface layers. This technology offers control over shaping the functional properties of materials being processed. FSP consists in heating and plasticising a material (parent metal) as a result of friction with a tool, provided (or not) with a probe, rotating and moving along an element surface subjected to processing. This method originates from the technology of friction stir welding (FSW), yet in comparison with this method, the phenomena taking place in the interface between the stirring area and the parent metal will have a decisive effect on the functional properties of a layer obtained through this process. The application, the course of the process, as well as the applied tools and equipment were discussed in the previous work [1]. The research of the friction stir processing (FSP) of surface layers, so far has

been focused mainly on the metallurgical analysis of microstructural changes in modified aluminium alloys [2-7]. Today's state of FSW/P (Friction Stir Welding/ Friction Stir Processing) research is described in the publication [8]. However, from a practical point of view it is important to determine the impact of FSP conditions, i.e. a tool rotational speed, travel rate, pressure force as well as the shape and type of tool on the moment acting on the tool, temperature in the stirring area, and the amount of heat generated in the stirring area. The heat generated in the area being processed and the level of plastic strain are factors having a decisive effect on microstructural changes, and, consequently, on the mechanical and functional properties of newly formed areas.

Determining dependences between the FSP process conditions will enable better understanding of physical phenomena accompanying a modification area formation process. These dependences can be determined experimentally, through the application of analytical models and by means of numerical calculations.

### Analytical and numerical models

On the basis of reference publications, the analytical models by means of which one calculates the amount of heat generated during FSW/P processes (Friction Stir

---

Marek St. Węglowski PhD Eng. - Instytut Spawalnictwa, Zakład Badań Spawalności i Konstrukcji Spawanych / Testing of Materials Weldability and Welded Constructions Department; Carter Hamilton - Miami University, School of Engineering and Applied Science, Oxford, Ohio, USA.

Table 1. Analytical models for the calculation of heat amount generated during FSW/P [9]

Model	Dependences describing the amount of generated heat	References
Frigaard Friction phenomena between the shoulder and the parent metal	$Q = \frac{2\pi}{3} \mu F \omega R_0^3$ $F = \frac{F_N}{\pi R_0^2}$	[14]
Chao and Qi Radial heat flux	$q(r) = \frac{3Qr}{2\pi(R_0^3 - R_1^3)}$ ; $R_0 \leq r \leq R_1$	[15, 16]
Colegrove Friction phenomena between the shoulder and the probe and the parent metal	Shoulder $\rightarrow Q = \frac{2\pi}{3} \mu F \omega (R_0^3 - R_1^3)$ ; $F = \frac{F_N}{\pi R_0^2}$ Probe $\rightarrow Q = 2\pi R_1 h \bar{Y} \frac{V_m}{\sqrt{3}} + \frac{2\pi \mu \bar{Y} R_1 h V_{RP}}{\sqrt{3(1-\mu^2)}} + \frac{4F\mu V_m \cos \Theta}{\pi}$ $V_m, V_{RP}$ and $\theta$ are experimental functions and can be expressed as: $\Theta = 90^\circ - \lambda - \arctan(\mu)$ ; $V_m = \frac{\sin \lambda}{\sin(180^\circ - \Theta - \lambda)}$ ; $V_{RP} = \frac{\sin \Theta}{\sin(180^\circ - \Theta - \lambda)} R_2 \omega$ $\lambda$ – angle of the thread of a spiral thread cut on the probe	[17, 18]
Schmidt, Hattel Model utilising phenomena of friction and strain	$Q_{total} = \delta Q_{viscous} + (1-\delta) Q_{dry}$ $\delta$ - non-dimensional coefficient indicating the type of friction between the tool surface and the parent metal	[12]
Reynolds, Hamilton	$Q_{total} = M_{total} \omega$	[19-25]
$Q$ - heat, $q$ - heat flux, $R_0$ - shoulder radius, $R_1$ - probe radius	$\mu$ - friction coefficient, $M$ - moment, $F$ - force [Pa] $F_N$ - force [N]	

Welding / Friction Stir Processing) can be classified into three groups [9], i.e. models based on the following:

- friction phenomenon [7, 10],
- plastic strain phenomenon [11],
- friction and plastic strain phenomena occurring at the same time [11, 12].

The first group of models is based on a theory that the main source of heat generated in the stirring area is the friction between the surface of a tool (shoulder, probe surface) and a parent metal. The second group contains models based on a theory stating that the

heat generated in the stirring area is the result of a strong plastic strain (deformation of the primary material structure caused by stirring with a tool). The third group combines both previous ones and is based on combined theories related to friction and plastic strain phenomena. Exemplary analytical equations of the models mentioned above are presented in Table 1.

Frigaard [14] proposed a model considering only friction phenomena i.e. the phenomena taking place during classical friction welding, with a constant heat flux under the

shoulder surface and without the effect of the probe. Chao [15, 16] expanded a model utilising a heat flux by taking into consideration the radial distribution for the density of a heat flux. Colegrove [17, 18] presented an analytical equation for the amount of heat generated by the probe, demonstrating that this heat can make up even 20% of the total generated heat. A limitation of the models presented above is the proper estimation of the friction coefficient  $\mu$ , which depends on temperature. The analytical dependences describing the models based on the assumption that the main source of generated heat is a plastic strain, do not differ significantly from the dependences related to friction phenomena. In these models, the product  $\mu F$  was replaced by a shearing stress [17, 18]. Schmidt and Hattel [12] introduced a model considering both friction and plastic strain phenomena, depending on whether the friction present is viscous or dry. In the dry friction, the tool pressure force, and thus the stress caused by it, is smaller than the stress of a strain at a given temperature. Therefore, the friction between the tool and the parent metal is the main source of heat. When the parent metal starts to conglomerate with the tool, the phenomenon of internal friction, being the source of heat, comes into being. Such assumptions are consistent with the assumptions proposed by Reynolds [19], who associates the amount of generated heat directly with the value of the moment acting on the tool. The same model was used by Hamilton in his deliberations [20-25].

Russell and Shercliff [26] used the Rosenthal's classical equation [27] (point source) in the analytical form to calculate temperature fields, assuming that a plastic strain during the FSW process occurs at a constant shear stress  $\tau$  (5% of a yield point at a room tempe-

rature), which is a result of the motion of plasticised material masses. Such an assumption enabled a relatively accurate determination of temperature fields only in the area located outside the shoulder (e.g. in the Heat Affected Zone).

In the simplest case the process of FSP at a given moment  $t_0$  can be treated as a rotational friction welding process. With such an approach one considers the heat flux density in the stirring area during the process of modification. The starting point for the calculation is the assumption that, at a given moment  $t_0$ , phenomena taking place between the tool without the probe and the surface being processed are the same as during friction welding.

During FSP, on the elementary surface  $ds$  ( $ds=2\pi r dr$ ) a heat flux  $dQ$  is generated. The flux can be presented as [28, 29] the following:

$$dQ = 2\pi \times r dr \times \mu \times p \times 2\pi \times \omega \times r = 4\pi^2 \times r^2 \times \mu \times p \times \omega dr \quad (1)$$

In view of the foregoing, in relation to the whole friction area, the total density of the heat flux amounts to

$$Q'' = \frac{dQ}{2\pi r dr} = 2\pi \cdot \mu \cdot p \cdot \omega \cdot r \quad (2)$$

where:

$Q$  – total heat flux generated on the surface under modification,

$r$  – radius of an element under discussion on the surface under modification,

$p$  – unitary pressure [MPa],

$\mu$  – friction coefficient,

$\omega$  – rotational speed [rev./min].

A friction coefficient is an unknown quantity, dependent on the rotational speed, unitary pressure and the distance from the rotation axis ( $\mu=f(\omega, p, r)$ ). In order to simplify calcu-

lations it was assumed [7], that on the whole friction area the product  $\mu \times p$  is constant. Therefore, if  $\mu \times p = \text{const}$ , then, by integrating equation 1 we obtain the following:

$$\int_0^R dQ = \frac{4}{3} \pi^2 \cdot \mu p \cdot \omega \cdot R^3 \quad (3)$$

where  $R$  signifies the FSP tool radius [m].

Generated thermal power must be equal to supplied friction power, which can be calculated from the friction moment and rotational speed:

$$Q = N_t = M \times 2\pi \times \omega \quad (4)$$

Comparing equations 3 and 4 we can see that

$$\mu p = \frac{3M}{2\pi R^3} \quad (5)$$

And, substituting equation 5 to 2, we obtain a simplified expression for the total density of a heat flux generated on a surface being processed:

$$Q'' = \frac{3M \cdot \omega \cdot r}{R^3} \quad (6)$$

However, due to the fact that the tool rotates and moves along a pre-defined trajectory, it is necessary to calculate the density of a heat flux for  $r=R$ . For this reason and taking into account necessary units, the obtained equations is as follows:

$$Q'' = \frac{3M \cdot \omega}{60 \cdot R^2} \left[ \frac{W}{m^2} \right] \quad (7)$$

where:

- $\omega$  – tool rotational speed [rev./min],
- $M$  – moment acting on the tool [Nm],
- $R$  – tool radius [m].

The above deliberations do not take into consideration the fact that the friction coefficient depends on temperature and decreases as temperature rises. They also do not take into account the fact that the exchange of generated heat in the friction area (tool surface – material being processed) takes

place between a rotating element (tool) and a plate (parent metal).

On the basis of reference publications of FSW/P research, it is noticeable that most authors, while calculating the value of generated thermal energy, use the Reynolds model which combines the value of heat generated in the stirring area with the moment acting on the tool. According to this model the value of thermal energy is directly proportional to the product of the total moment and rotational speed [19]:

$$Q_{total} = M_{total} \omega \quad (8)$$

In turn, the total moment acting on the tool can be expressed by the following dependence [19, 30]:

$$M_{total} = M_{shoulder} + M_{probe\ side} + M_{probe\ end} \quad (9)$$

where:

- $M_{shoulder}$  – moment resulting from the action of the shoulder on a processed material,
- $M_{probe\ side}$  – moment resulting from the action of the probe side surface on a processed material,
- $M_{probe\ end}$  – resulting from the action of the probe end face on a material being processed.

In the most generalised case, one could consider a tool with a conical probe and a concave shoulder. Figure 1 presents the scheme of such a tool along with characteristic quantities used in the calculations.

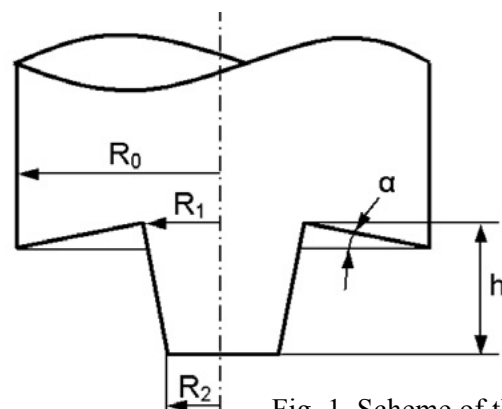


Fig. 1. Scheme of the FSW/P tool

On the basis of the above deliberations one can write that [12]:

$$M_{shoulder} = \int_0^{2\pi} \int_{R_1}^{R_0} r^2 (1 + \tan \alpha) dr d\Theta = \frac{2}{3} \pi \tau (R_0^3 - R_1^3) \cdot (1 + \tan \alpha) \quad (10)$$

$$M_{probeside} = \int_0^{2\pi} \int_0^h \tau \left( \frac{R_2 - R_1}{2} \right)^2 dz d\Theta = 2\pi \tau \left( \frac{R_2 - R_1}{2} \right)^2 \cdot h \quad (11)$$

$$M_{probe\ end} = \int_0^{2\pi} \int_0^{R_2} \tau R_2^2 dr d\Theta = \frac{2}{3} \pi \tau R_2^3 \quad (12)$$

where:

$R_0$  – shoulder radius,

$R_1$  – probe radius near the shoulder,

$R_2$  – probe radius near the face,

$\tau$  – average shear stress,

$h$  – probe length.

Therefore, after transformations the total moment can be expressed by the following equation:

$$M_{total} = \frac{2}{3} \pi \tau \left[ (R_0^3 - R_1^3) \cdot (1 + \tan \alpha) + 3 \left( \frac{R_1 - R_2}{2} \right)^2 \cdot h + R_2^3 \right] \quad (13)$$

This research-related work will require the use of a tool with a flat shoulder. For this reason the total moment can be expressed as:

$$M_{total} = \frac{2}{3} \pi \tau \left[ R_0^3 - R_1^3 + R_2^3 + 3 \left( \frac{R_1 - R_2}{2} \right)^2 \cdot h \right] \quad (14)$$

If, additionally, one uses a cylindrical probe ( $R_1 = R_2$ ), then [21]:

$$M_{total} = \frac{2}{3} \pi \tau [R_0^3 + 3R_1^2 \cdot h] \quad (15)$$

Hamilton [21] states that a shear stress can be expressed as:

$$\tau = \frac{\mu \cdot F}{\pi \cdot R_0^2} \quad (16)$$

where:

$\mu$  – coefficient of friction between the tool surface (tool steel) and the parent metal (aluminium alloy),

$F$  – pressure force.

This assumption is right if Coulomb's law was taken into consideration as well as if it was taken into account that the friction taking place between the bodies involved in the process is sliding friction.

Schmidt [12] states that if viscous friction occurs, the value of a shear stress can be expressed as the following:

$$\tau = \tau_{plastic} = \frac{\sigma_{plastic}}{\sqrt{3}} \quad (17)$$

$\tau_{plastic}$  – shear stress occurring at a yield point,

$\sigma_{plastic}$  – normal stress occurring at a yield point.

Simplifying the deliberations one obtains [21]:

$$M_{total} = 2\mu F \left[ \frac{1}{3} R_0 + \frac{R_1^2}{R_0^2} \cdot h \right] \quad (18)$$

Therefore, the average value of generated heat can be calculated as:

$$Q_{average} = 2\mu F \left[ \frac{1}{3} R_0 + \frac{R_1^2}{R_0^2} \cdot h \right] \cdot \omega \quad (19)$$

and linear energy as:

$$E = \frac{Q}{v} = M_{total} \frac{\omega}{v} \quad (20)$$

A problem is how to select the proper value of the friction coefficient. A friction coefficient between the aluminium (test plate) and the steel (tool) depends on the temperature of the stirring area, which in turn, depends on the process conditions. When the temperature reaches the value of the solidus temperature for a given alloy, the area of distribution between the shoulder and the material being processed effectively reduces the friction coefficient [14]. Frigaard and his team adopted a friction coefficient between aluminium and steel to be 0.4. It should also be noticed that in the previous tests [31] a friction coefficient adopted for viscous friction was 0.5, and for dry friction [14] amounted to 0.25. Soundarajan [32] adopted a friction coefficient be-

tween 0.4 and 0.5; it was also assumed that this coefficient decreased along with an increase in the stirring area temperature. Hamilton in his research adopted a coefficient  $\mu=0.5$  for all tested FSW process conditions [21].

During testing FSW/P it was also important to determine the real mechanical properties of the parent metal. It is known that increasing the rotational speed of the tool leads to a higher temperature of the material directly under the surface of the tool [17].

One of the methods making it possible to determine the real yield point in the material subjected to strong plastic strains at a heightened temperature is the Johnson-Cook constitutive model [33]:

$$\sigma_y = \left( A + B[\epsilon^{pl}]^n \right) \left( 1 + C \ln \frac{\dot{\epsilon}^{pl}}{\dot{\epsilon}_0} \right) \left( 1 - \left( \frac{T - T_{ref}}{T_m - T_{ref}} \right)^m \right) \quad (21)$$

where:

$\sigma_y$  – reduced plastic stress of the flow,

$\epsilon^{pl}$  – reduced plastic strain,

$\dot{\epsilon}^{pl}$  – reduced rate of the plastic strain,

$\dot{\epsilon}_0$  – reference rate  $1 \text{ s}^{-1}$ ,

A – yield point,

B, n – strengthening parameters,

C – parameter of sensitivity to the rate of strain,

T – temperature for which  $\sigma_y$  is determined,

$T_m$  – melting point,

$T_{ref}$  – initial temperature – 294 K,

m – exponent of thermal plasticisation.

The work [21] based on this model and researcher's own calculations reveals a significant impact of temperature on the value of a yield point for FSW of aluminium alloy grade 6061. The results are presented in Figure 2.

One of the methods enabling the analysis of physical phenomena taking place during stirring is the application of reverse engineering and the development of a mathematical model based on this engineering. Such a solution was adopted by P. Vilaca [13, 34], who developed a model enabling, among others, the calculation of a thermal efficiency coefficient, thermal power and temperature distribution around the probe taking into consideration FSW process conditions. The authors [13, 34] created a software application iSTIR enabling the generation of both 2D and 3D models. Input data related to temperature fields are a result of measurements carried out using a thermographic camera.

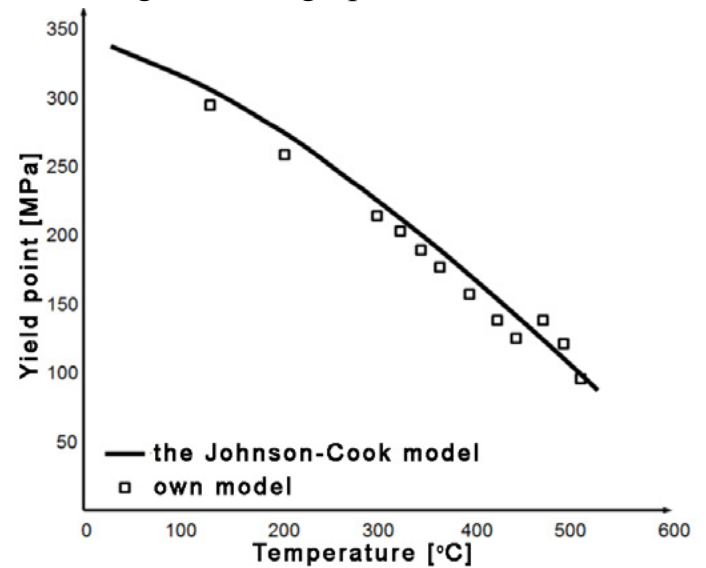


Fig. 2. Results of yield point calculations for aluminium alloy grade 6061 based on the Johnson-Cook model [21]

A thermal efficiency coefficient can be expressed as the following [13]:

$$\eta_{therm} \left( \frac{\omega}{v}; F_z \right) = \left( 1 - \frac{P_{therm}}{P_{mech}} \right) \cdot 100\% \quad (22)$$

where:

$\omega$  – rotational speed [rev./min],

v – travel rate [mm/min],

$F_z$  – pressure force [kN],

$P_{therm}$  – generated thermal power [W],

$P_{mech}$  – mechanical power [W].

Mechanical power can be calculated from the following dependence:

$$P_{\text{mech}} = M_z \cdot \frac{2\pi}{60} \omega + F_x + \frac{0,001}{60} v \quad (23)$$

where:

$M_z$  – moment [Nm],

$F_x$  – force in the tool travel direction [N].

The authors [13] pointed out that during the analysis of the FSW process it is important to take into consideration the relation between the rotational speed and the travel rate. The relation between these two types of speeds has a decisive effect on the amount of heat generated during FSW/P. When temperature is the measure of the amount of generated heat, one can speak of high-, medium- and low-temperature parameters:

$\frac{\omega}{v} > 4$  – high-temperature parameters,

$2 \leq \frac{\omega}{v} \leq 4$  – medium-temperature parameters,

$\frac{\omega}{v} < 2$  – low-temperature parameters.

The above boundary values are the result of the analysis carried out on the basis of metallographic test results (stirring area geometry), hardness measurements and measurements of temperature fields. Differences appear in the heat flow; during the production of a joint with parameters ensuring small amounts of generated heat, the heat is mainly emitted by viscous dissipation (internal friction) triggered by the plastic strain connected with the rotation of the probe and squeezing the material accumulated around the probe onto the retreating side. For the parameters ensuring a great amount of heat generated as a result of inter-phase friction between the parent metal and the tool during FSW and FSP, a greater plastic strain is located closer

to the probe. The generated heat is located almost symmetrically both on the advancing and the retreating side.

The authors [34] assumed that physical properties, i.e. density, specific heat and conductance ratio do not depend on temperature. According to the authors such an assumption does not significantly affect the error of values being determined. The authors also assumed the point model of the heat source, which translated to a shorter calculation time and easier visualisation of test results. On the basis of the calculated values of thermal power it was possible to calculate linear energy using the dependence:

$$E = \frac{P_{\text{therm}}}{v} \cdot 60 \quad (24)$$

On summing up the overview of reference publications related to FSP tests one can state that the so-far research has been focused on creating analytical dependences and that experimental verification was carried out only for selected (narrow) FSP parameters. The purpose of the work was to determine the impact of FSP technological parameters on the moment and temperature as well as to create a numerical thermal model, the results of which were compared with the data obtained experimentally.

## Test methodology and materials

FSP was tested by means of an FSW station located at Instytut Spawalnictwa in Gliwice. The station was composed of a conventional milling machine FYF32JU2, system for fixing test plates and a measurement head LOWSTIR (LOWSTIR - LOW cost processing unit for Friction Stir Welding) (Fig. 3a). The tests were carried out using a tool with a shoulder of a 20 mm diameter, a probe with a diameter of 8 mm and a length of 4 mm

(Fig. 3b). The tool was made of high speed steel grade H6-5-2. The tests were conducted on a 6 mm-thick test plate made of aluminium casting alloy AlSi9Mg, using 27 technological parameters. The technological parameters were selected on the basis of previous experiments related to the FSW process and the milling machine operating range (FYF32JU2). The field of FSP parameters is presented in Figure 4.

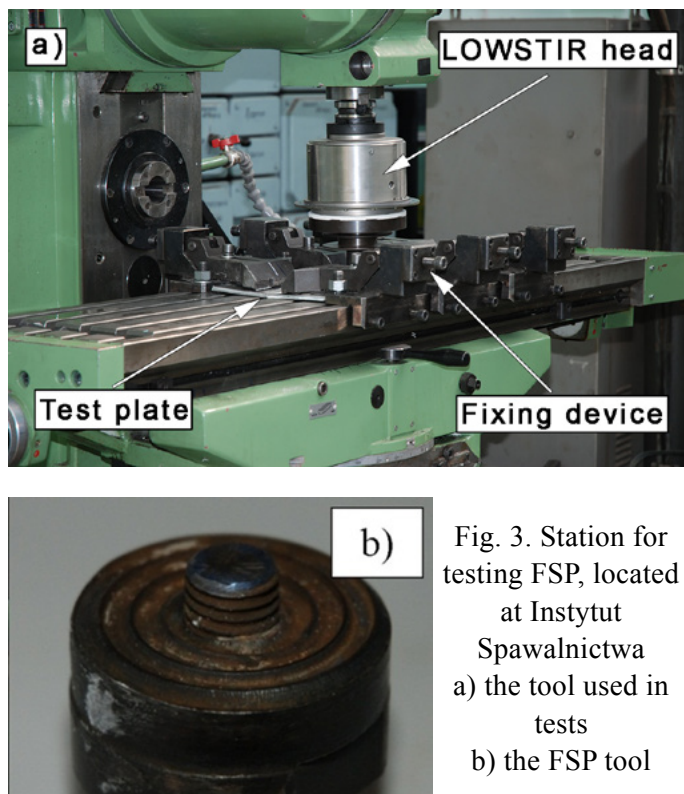


Fig. 3. Station for testing FSP, located at Instytut Spawalnictwa  
 a) the tool used in tests  
 b) the FSP tool

Due to the device's limitations, the maximum available travel rate of the tool was 1120 mm/min. The minimum rate under consideration was 112 mm/min. Lower values of the travel rate were not taken into account due to the low efficiency of the process itself.

The technological tests involved the measurements of the moment and forces by means of a LOWSTIR measurement head. The measurements were registered during the processing of the test plate surface along a 150mm-long section, at a frequency of 100 Hz. The average value of the moment for

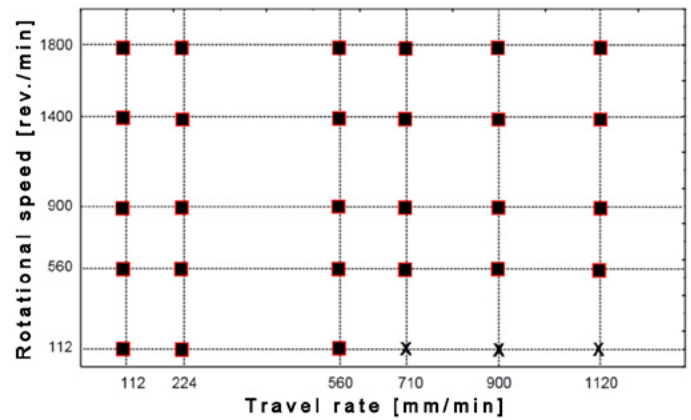


Fig. 4. Field of FSP parameters, x – parameters for which the power of the device was insufficient

each experiment was calculated out of 100 measurement points. The area considered was the one where the complete FSP stabilisation took place (Fig. 5). The value of the moment used in the calculations was an average value based on three experiments.

Temperature measurements in the stirring area were conducted by means of a system utilising a TempSTIR head. For each set of parameters the measurements were carried out three times. At that stage of the tests it was assumed that the tool temperature corresponded to the temperature in the stirring area. The analysis of measurement data was carried out using Origin Pro software ver. 8.5 (function matching) and in the Statistica environment ver. 10. The thermal model of the FSP was developed using the Comsol Multiphysics software.

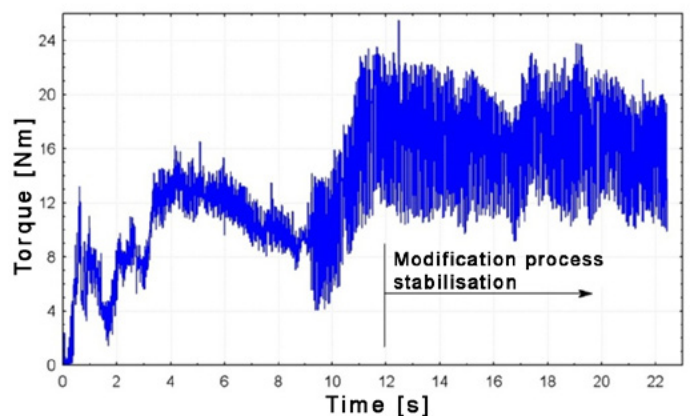


Fig. 5. Exemplary course of the torque acting on the tool during FSP,  $\omega=900$  rev./min,  $v=710$  mm/min

## Test results and discussion

The tests involved the measurements of the impact of FSP parameters on the torque acting on the tool, the tool temperature, the amount of generated heat and a friction coefficient. The experimental data were compared with the results of numerical calculations. An exemplary course of the torque is presented in Figure 5. Figure 6 presents the impact of the rotational speed of the FSP tool on the moment acting on the tool at a constant travel rate, for selected sets of parameters. Figure 7 presents the impact of the travel rate of the FSP tool on the moment acting on the tool at a constant rotational speed. In order to test the impact of the tool rotational speed on the torque value, the obtained results were approximated using a function  $y=a \times \exp(-x/b)+c$ . The function applied for the travel rate was  $y=a \times x+b$ . As can be seen in Figure 6, the rotational speed of the tool strongly affects the torque. An increase in the rotational speed leads to a decrease in the torque. This phenomenon is caused by the fact that an increase in rotational speed causes an increase in the temperature of the material (parent metal) being processed, and consequently a decrease in the coefficient of friction in the parent metal.

Using the dependence (8) it was possible to calculate the amount of the heat generated in the stirring area. The results are presented in Figure 8. As can be seen, an increase in the rotational speed to 900 rev./min results in an increase of generated heat, followed by its slight decrease. This phenomenon can be explained by the fact that an increase in the rotational speed is accompanied by a decrease in the volume and the mass of material

being processed[5], which, in turn, leads to a decrease in generated heat, according to the following dependence (8):

$$Q = mc \Delta T \quad (25)$$

where:

Q – generated heat,

m – mass of stirred material,

$\Delta T$  – temperature change,

c – specific heat.

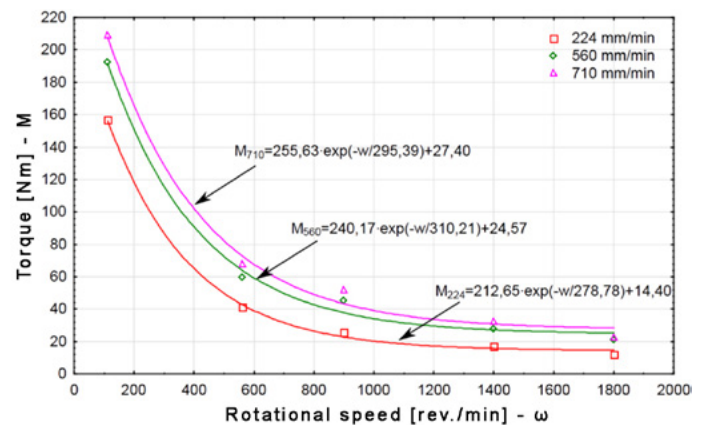


Fig. 6. Impact of the FSP tool rotational speed on the moment acting on the tool at a constant travel rate

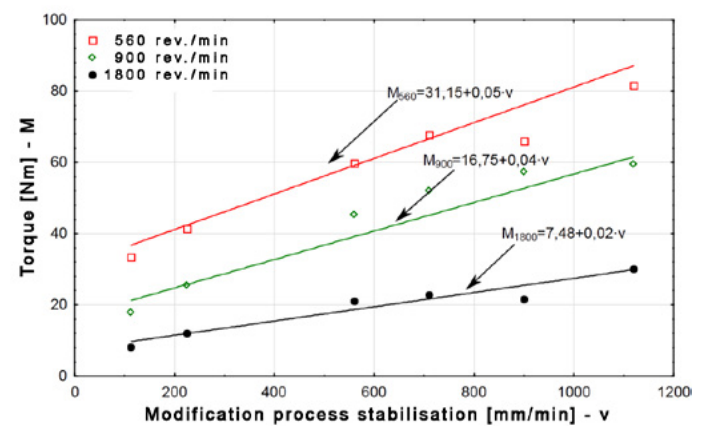


Fig. 7. Impact of the FSP tool travel rate on the torque acting on the tool at a constant rotational speed

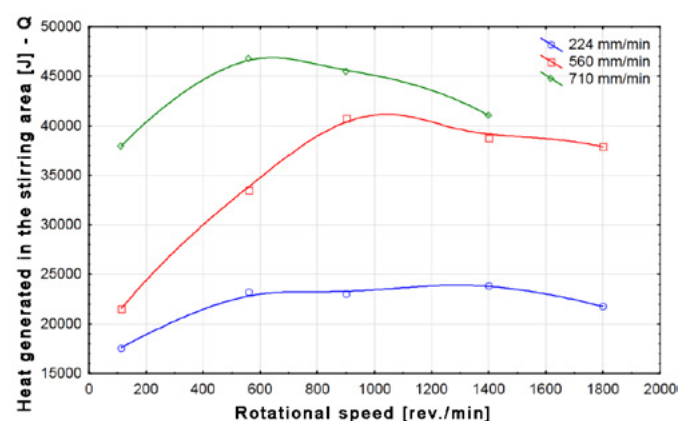


Fig. 8. Impact of rotational speed on the amount of heat generated in the stirring area

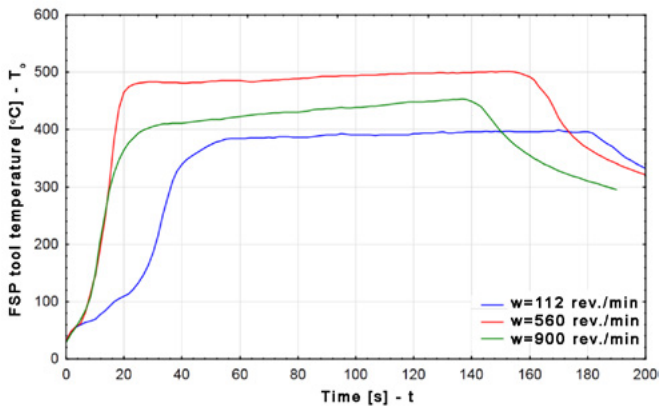


Fig. 9. Course of temperature changes in the tool during surface modification at a constant travel rate  $v=112$  mm/min

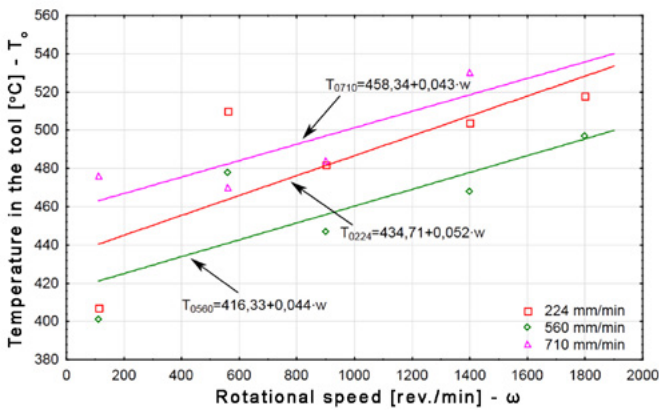


Fig. 10. Impact of rotational speed at constant travel rate on FSP tool temperature

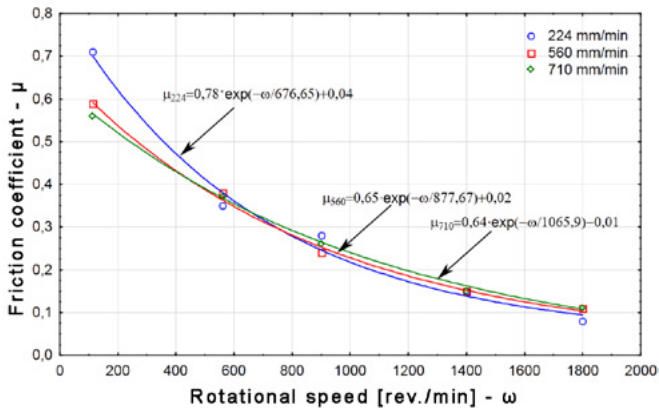


Fig. 11. Impact of rotational speed (temperature in Fig. 10) on the friction coefficient calculated from the dependence (18)

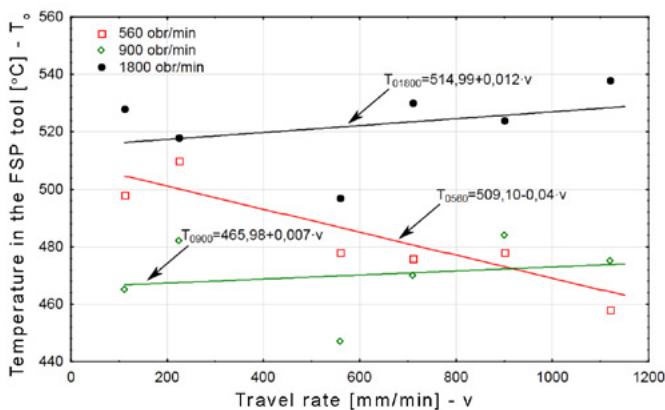


Fig. 12. Impact of travel rate at constant rotational speed on FSP tool temperature

The temperature of the FSP tool was measured using a temperature sensor located approximately 1 mm away from the work surface of the tool. Figure 9 presents an exemplary course of the tool temperature during the process of modification.

It is also important to determine how FSP parameters (rotational speed and travel rate) affect the value of temperature in the stirring area. Figure 10 presents the impact of the rotational speed at a constant travel rate on the value of the maximum temperature directly after the completion of the modification process (stopping the plane motion of the tool). As can be seen, an increase in the rotational speed causes an increase in the stirring area temperature. This is due to the fact that an increase in the rotational speed is accompanied by a decrease in the volume and the mass of a material being processed [5]. As a result, heat is generated in a smaller volume, which leads to an increase in temperature according to the dependence (25).

The dependence (18) was used to calculate the value of the coefficient of friction between the tool surface and the material being processed. The impact of the rotational speed on the value of the friction coefficient is presented in Figure 11. The decrease in the friction coefficient along with the increase in the rotational speed is caused by the increase in temperature in the stirring area (tool temperature) (Fig. 10). Figure 12 presents the impact of the tool travel rate, at a constant rotational speed, on the value of temperature.

The results of temperature measurements are compatible with the results of moment measurements (Fig. 6 and 7). An increase in the tool rotational speed causes a temperature increase in the stirring area (Fig. 10)

and the reduction of the friction coefficient, and thus an decrease in the torque (friction moment). In turn, an increase in the travel rate does not cause such significant changes either in the temperature (Fig. 11) or in the moment (Fig. 9).

Using the thermal model developed for the FSW process [23] a new numerical model was developed. The model was created using the Comsol Multiphysics computational environment. Similarly, as in the previous model, it was necessary to adopt certain simplifications. For instance, it was assumed that heat was generated only by the friction between the surface of the tool and the material being processed. The calculations did not take into account the impact of the plastic strain on the amount of generated heat. On the basis of these assumptions, the heat generated between the tool and the material can be expressed as:

$$q = \delta_E \mu P_N (\omega r - v_x \sin \Theta) \quad (26)$$

where:

$\delta_E$  – slip ratio,

$\mu$  – coefficient of friction between the FSP tool and the surface of the material,

$P_N$  – pressure exerted by the tool on the material being processed,

$\omega$  – tool rotational speed,

$r$  – distance between the tool axis and a tool surface fragment under consideration,

$v_x$  – tool travel rate,

$\Theta$  – angle between the tool axis and a fragment under consideration.

The values of physical constants adopted for the calculations are presented in Table 2.

In the developed model, taking into consideration the tool used during the experimentation, three areas generating heat during mo-

dification were taken into account (Fig. 13):

- shoulder surface  $q_1$ ,
- probe side surface  $q_2$ ,
- probe end face  $q_3$ .

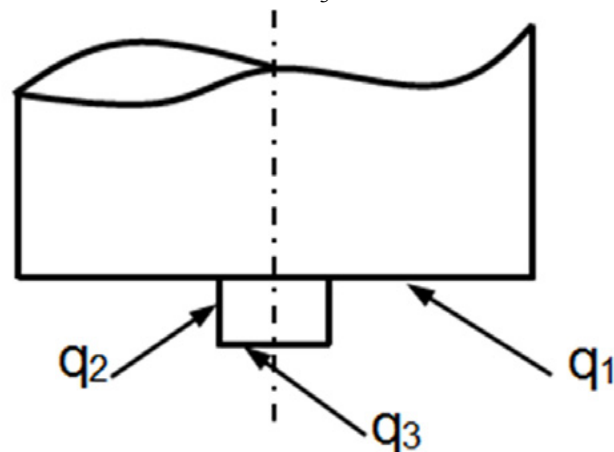


Fig. 13. Schematic presentation of generated heat components

Taking into consideration typical conditions taking place during FSW, normal force acting on the tool probe, i.e. the force in the direction of welding, is significantly lower than the force acting on the shoulder and the face part of the probe. The pressure force, from the generated heat point of view, is negligible. However, during FSP, normal pressure exerted on the probe (see equation 26) is significant and may constitute from 20 to 50% of the pressure acting on the shoulder. It is of particular importance in the case of high values of travel rate (900 and 1120 mm/min). Taking into consideration the phenomena taking place in the tool – material interface, while modelling FSP one must take into consideration three heat fluxes (Fig. 13).

Table 2. Values of physical constants adopted for the calculations

Constant	Value
Density	2670 [kg/m <sup>3</sup> ]
Thermal capacity	963 [J/kgK]
Thermal conductivity	138 [W/mK]
Melting point	835.8 [K]
Yield point	276 [MPa]
Modulus of elasticity	70 [GPa]
Thermal diffusivity	5.37×10 <sup>-5</sup>

Higher tool travel rates occurring during FSP (in comparison with the classical FSW process) cause that the expression  $v_x \sin \Theta$  cannot be omitted. During the FSW process the expression  $\omega r$  is usually significantly greater than  $v_x \sin \Theta$ , and that is why the expression  $v_x \sin \Theta$  is negligible. For this reason, in the case under consideration, the angle  $\Theta=90^\circ$  will be adopted in equation 26 and the average heat generated between the shoulder surface and the material will be taken into account in calculations. Therefore, the equations describing the fluxes of generated heat will take the following form:

$$q_1 = \frac{\int_{r_{probe}}^{r_{shoulder}} \int_0^\theta \delta_E \mu P_N (\omega r - v_x) r dr d\theta}{\pi r_{shoulder}^2 - \pi r_{probe}^2} = \delta_E \mu P_N \left( \frac{2}{3} \omega \frac{r_{shoulder}^3 - r_{probe}^3}{r_{shoulder}^2 - r_{probe}^2} - v_x \right) \quad (27)$$

$$q_2 = \frac{\delta_E \mu P_N (\omega r_{probe} - v_x)}{2\pi r_{probe} h_{probe}} \quad (28)$$

$$q_3 = \frac{\int_0^{r_{probe}} \int_0^\theta \mu P_N (\omega r - v_x) r dr d\theta \delta_E}{\pi r_{probe}^2} = \delta_E \mu P_N \left( \frac{2}{3} \omega r_{probe} - v_x \right) \quad (29)$$

where:

- $r_{probe}$  – probe radius,
- $r_{shoulder}$  – shoulder radius,
- $h_{probe}$  – probe height.

The numerical calculations involved an assumption that FSP stabilises after approximately 10 seconds following the beginning of the tool motion. At the initial stage, before the process stabilisation, pressure forces, the forces in the direction of travel and the moment increase, approximately, linearly. Taking into consideration the fact that the heat fluxes under consideration are directly proportional to normal forces, the linear dependence (an increase in the moment value

in the function of time) was taken into account for the heat fluxes in the thermal model only for time below 10 seconds. After 10 s, i.e. after the stabilisation of the process, heat fluxes were calculated in accordance with equations 27-29. In order to shorten the time of calculations the simulation was calculated for the process duration up to 30 seconds. An exemplary result of numerical calculations is presented in Figure 14.

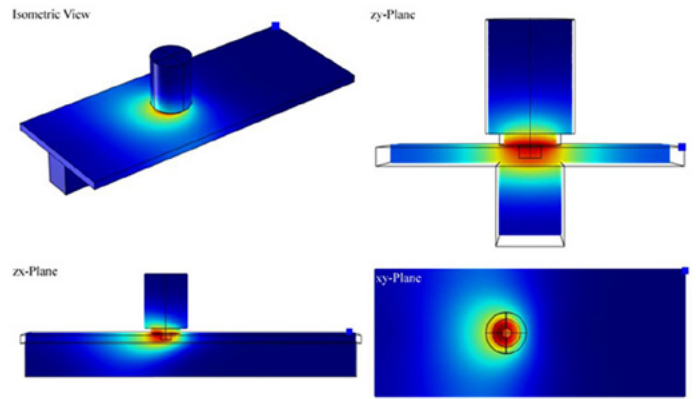


Fig. 14. Exemplary result of numerical calculations in the Comsol Multiphysics programme

An exemplary comparison of the numerical calculations with the experimental data is presented in Figure 15. The calculated temperatures undergo changes comparable with the real temperatures measured in the tool by means of the TermSTIR head. The results of temperature calculations indicate that the calculated temperature slightly differs from the real temperature in the probe. This is most probably due to the simplifications carried out in the numerical model (the

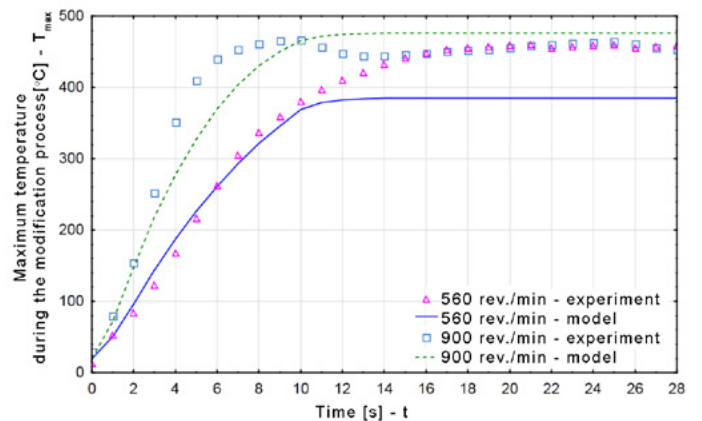


Fig. 15. Comparison of numerical calculation results with experimental data, travel rate 710 mm/min

impact of the heat generated as a result of the strong plastic deformation of the material being processed was not taken into consideration), which have a greater impact in the case of lower travel rate values. It is also obvious that the temperature in the tool itself will slightly differ from the temperature in the stirring area due to the heat being carried off by the tool holder.

## Conclusions

On the basis of the conducted investigation it is possible to formulate the following conclusions:

- increase in the tool rotational speed causes a decrease in the moment acting on the tool,
- increase in the travel rate causes slight changes of torque values,
- increase in the rotational tool to 900 rev./min causes an increase in the amount of generated heat and its slight decrease afterwards,
- increase in the rotational tool causes an increase in the stirring area temperature, and thus a decrease in the friction coefficient,
- increase in the travel rate causes a decrease in the tool temperature or a slight increase in the moment,
- results of the numerical calculations coincide with the experimental data.

***The research was carried out within the statutory activity at Instytut Spawalnictwa and financed by the Ministry of Science and Higher Education.***

## References

1. Węglowski M.St.: Technologia Friction Stir Processing – nowe możliwości. Biuletyn Instytutu Spawalnictwa, 2011, nr 2, s. 25-31

2. Ma Z.Y.: Friction Stir Processing Technology: a review. Metallurgical and Materials Transactions A, 2008, t. 39a, s. 642-658.

3. Mishra R.S.: Friction stir welding and processing. Materials Science and Engineering R: Reports, 2005, t. 50, s. 1-78

4. Lohwasser D., Chen Z.: Friction stir welding: From basics to applications, Woodhead publishing, Cambridge, 2009.

5. Węglowski M.St., Dymek S.: Microstructural modification of cast aluminium alloy AlSi9Mg via Friction Processed Processing. Archives of Metallurgy and Materials, 2012, t. 57, nr 1, s. 71-78

6. Mroczka K., Dutkiewicz J., Pietras A.: Microstructure of friction stir welded joints of 2017A aluminium alloy sheets. Journal of Microscopy-Oxford, 2010, t. 237, s. 521-525

7. Węglowski M., Łomozik M., Krasnowski K., Kwieciński K., Jachym R., Rams B.: Badanie procesu stopowania mechanicznego warstw wierzchnich stopów aluminium oraz wyznaczenie temperatur krytycznych przemian austenitu w stalach konstrukcyjnych na multipomiarowym stanowisku badawczym. Instytut Spawalnictwa, praca badawcza nr Id – 137 (ST 274), 2010

8. Lohwasser D., Chen Z.: Friction stir welding. From basics to application, Woodhead publishing, Cambridge, 2009

9. Attallah M.M.: Microstructure property development in friction stir welds of aluminium based alloys. Praca doktorska University of Birmingham, 2007

10. Song M., Kovacevic R.: Numerical and experimental study of the heat transfer process in friction stir welding. Proceedings of the Institution of Mechanical Engineers, Part B: Journal of Engineering Manufacture, 2003, t. 217, s. 73-85

11. Simar A., Pardoën T., Meester B.: Influence of the friction stir welding parameters on the power input and temperature distribution in Aluminium alloys. 5th International Symposium on Friction Stir Welding, Metz, France, 2004
12. Schmidt H., Hattel J., Wert J.: An analytical model for the heat generation in friction stir welding. *Modelling and Simulation in Materials Science and Engineering*, 2004, t. 12, s. 143-157
13. Vilaca P., Quintino L., Santos J.F.: iSTIR – Analytical thermal model for friction stir welding. *Journal of Materials Processing Technology*, 2005, t. 169, nr 3, s. 452-465
14. Frigaard, Ø., Grong, Ø., Midling O.T.: A process model for friction stir welding of age hardening aluminium alloys. *Metallurgical and Materials Transactions A*, 2001, t. 32A, nr 5, s. 1189-1200
15. Chao Y.J., Qi X.: Heat Transfer and Thermo-Mechanical Modelling of Friction Stir Welding Joining of AA6061-T6 Plates. *First International Symposium on Friction Stir Welding*, Rockwell Science Center, Thousand Oaks, CA, 1999
16. Chao Y.J., Qi X., Tang W.: Heat transfer in friction stir welding-experimental and numerical studies. *Transactions of the ASME. Journal of Manufacturing Science and Engineering*, 2003, t. 125, s. 138-145
17. Shercliff H.R., Colegrove P.A.: Modelling of Friction Stir Welding. *Mathematical Modelling of Weld Phenomena*, Cerjak H., Bhadeshia H.K.H.D., Maney Publishing, London 2002, t. 6, s. 927-974
18. Colegrove P.A., Painter M., Graham D., Miller T.: 3-dimensional flow and thermal modelling of the friction stir welding process. *2nd International Symposium on Friction Stir Welding*, Gothenburg, Sweden, 2000
19. Reynolds A.P., Tang W., Khandkar Z., Khan J.A., Lindner K.: Relationships between weld parameters, hardness distribution and temperature history in alloy 7050 friction stir welds. *Science and Technology of Welding and Joining*, 2005, t. 10, nr 2, s. 190-199
20. Hamilton C., Dymek S., Kalembe I., Blicharski M.: Friction stir welding of aluminium 7136-T76511 extrusions. *Science and Technology of Welding and Joining*, 2008, t. 13, nr 8, s. 714-720
21. Hamilton C., Sommers A., Dymek S.: A thermal model of friction stir welding applied to Sc-processed Al-Zn-Mg-Cu alloy extrusions. *International Journal of Machine Tools & Manufacture*, 2009, t. 49, s. 230-238
22. Hamilton C., Dymek S., Blicharski M.: Friction stir welding of aluminium 7136-t76511 extrusions for aerospace applications, *Proceedings of IMECE2007 ASME International Mechanical Engineering Congress and Exposition*, 2007, s. 1-6
23. Hamilton C., Dymek S., Kalembe I., Blicharski M.: A Thermal Model of Friction Stir Welding Applied to Aluminium 7136-T76511 Extrusions. *TMS*, 2008, s. 33-40
24. Hamilton C., Dymek S., Blicharski M.: Friction stir welding of aluminium 7136-T76511 extrusions. *Archives of Metallurgy and Materials*, 2008, t. 53, nr 4, s. 1047-1054
25. Hamilton C., Dymek S., Sommers A.: A thermal model of friction stir welding in aluminium alloys. *International Journal of Machine Tools & Manufacture*, 2008, t. 48, nr 10, s. 1120-1130
26. Russell M.J., Shercliff H.R.: Analytical Modelling of Microstructure Development in Friction Stir Welding. *First International Symposium on Friction Stir Welding*, Rockwell Science Center, Thousand Oaks, CA, 1999

27. Rosenthal D.: The Theory of Moving Source of Heat and its Application to Metal Transfer. Transactions ASME, 1946, t. 43, s. 849-866
28. Ambrosia A.: Zgrzewanie tarciove metali trudno topliwych w cieczy na tle innych metod spajania. Oficyna Wydawnicza Politechniki Wroclawskiej, Wroclaw 1998
29. Krawczyk R.: Analiza procesu nagrzewania metali podczas zgrzewania tarciovego. Praca doktorska, Czestochowa 1993
30. Reynolds A., Khandkar Z., Long T.: Utility of relatively simple models for understanding process parameters effects on FSW. Materials Science Forum, 2003, t. 426-432, nr 4, s. 2959-2694
31. Midling O.T., Grong Ø.: A process model for friction welding of Al-Mg-Si alloys and Al-SiC metal matrix composites. Part I. HAZ temperature and strain rate distribution. Acta Metallurgica et Materialia, 1994, t. 42, nr 5, s. 1595-1609
32. Soundararajan V., Zekovic S., Kovacevic R.: Thermo-mechanical model with adaptive boundary conditions for friction stir welding of Al 6061. International Journal of Machine Tools and Manufacture, 2005, t. 45, nr 14, s. 1577-1587
33. Johnson G.R., Cook W.H.: A constitutive model and data for metals subjected to large strains, high strain rates, and high temperatures. Proc. 7th. Int. Symp. Ballistics, 1983, s. 541-547
34. Vilaca P., Quintino L., Santos J.F., Zettler R., Sheikhe S.: Quality assessment of friction stir welding joints via an analytical thermal model, iSTIR. Materials Science and Engineering A, 2007, t. 445-446, s. 501-508